Taylor & Francis
Taylor & Francis Group

New preclinical biomarkers for prion diseases in the cerebrospinal fluid proteome revealed by mass spectrometry

Sonia Pérez-Lázaro[a]*, Tomás Barrio[b]*, Susana B. Bravo[c], Eloisa Sevilla[a], Alicia Otero[a], María del Pilar Chantada-Vázquez[c], Inmaculada Martín-Burriel[d], Jesús R. Requena[e], Juan J. Badiola[a] and Rosa Bolea[a]

[a]Centre for Encephalopathies and Emerging Transmissible Diseases, Faculty of Veterinary Sciences, University of Zaragoza – Agri-Food Institute of Aragon (IA2), Zaragoza, Spain; [b]UMR Institut National de La Recherche Pour L'Agriculture, L'Alimentation Et L'Environment (INRAE), École Nationale Vétérinaire de Toulouse (ENVT) 1225 IHAP (Interactions Hôtes-Agents Pathogènes), Toulouse, France; [c]Proteomic Unit, Health Research Institute of Santiago de Compostela (IDIS), University Clinical Hospital of Santiago de Compostela (CHUS), Santiago de Compostela, Spain; [d]Laboratory of Genetics and Biochemistry (LAGENBIO), Faculty of Veterinary Sciences, University of Zaragoza – Agri-Food Institute of Aragon (IA2), Zaragoza, Spain; [e]CIMUS Biomedical Research Institute & Department of Medical Sciences, University of Santiago de Compostela-IDIS, Santiago de Compostela, Spain

ABSTRACT

Current diagnostic methods for prion diseases only work in late stages of the disease when neurodegeneration is irreversible. Therefore, biomarkers that can detect the disease before the onset of clinical symptoms are necessary. High-throughput discovery proteomics is of great interest in the search for such molecules. Here we used mass spectrometry to analyse the cerebrospinal fluid proteome in an animal prion disease: preclinical and clinical sheep affected with natural scrapie, and healthy sheep. Interestingly, we found 46 proteins in the preclinical stage that were significantly altered ($p < 0.01$) compared to healthy sheep, mainly associated with biological processes such as stress and inflammatory responses. Five of them were selected for validation by enzyme-like immunosorbent assay: synaptotagmin binding, cytoplasmic RNA interacting protein (SYNCRIP), involved in nucleic acid metabolism; phospholipase D3 (PLD3) and cathepsin D (CTSD), both related to lysosomal apoptosis; complement component 4 (C4), an element of the classical immune response; and osteopontin (SPP1), a proinflammatory cytokine. These proteins significantly increased in the preclinical stage and maintained their levels in the clinical phase, except for CTSD, whose concentration returned to basal levels in the clinical group. Further research is ongoing to explore their potential as preclinical biomarkers of prion diseases.

Introduction

Transmissible spongiform encephalopathies (TSE) or prion diseases are progressive and fatal neurodegenerative disorders that affect both animals and humans. This group of disorders includes various diseases in animals, such as bovine spongiform encephalopathy in cattle and scrapie in small ruminants, the latter being the first identified and most studied reference model of these diseases (McGowan 1922; Prusiner 1982). In humans, sporadic Creutzfeldt-Jakob disease (sCJD) is the most common type of prion disorder nowadays, with 1–2 cases per million per year worldwide (Mackenzie and Will 2017).

All of them are characterised by the accumulation of the pathological prion protein (PrPSc), mainly in the central nervous system (CNS). PrPSc is the abnormal isoform of a physiological membrane glycoprotein called cellular prion protein (PrPC) and it is the causal agent of these diseases and the only pathognomonic biomarker identified so far. Consequently, the confirmatory diagnosis of TSE is still based on *post mortem* histopathological observation of the characteristic spongiform lesions and detection of PrPSc using CNS tissue samples. However, in sheep scrapie, it is possible to diagnose the infection *in vivo* by the detection of PrPSc in lymphoid tissue through biopsies of rectal mucosa, third eyelid or tonsils since PrPSc can be distributed throughout the lymphoreticular system before reaching the CNS. This technique has certain limitations when used as a diagnostic procedure, due to the variability of the magnitude

and time of onset of lymphoid tissue involvement between different animals, genotypes of the gene encoding PrP^C or even prion strains; however, it can be considered 100% specific (Monleón et al. 2011).

The cerebrospinal fluid (CSF) is produced in the CNS and it is found to be in equilibrium with the brain and spinal cord, playing an essential role in maintaining the homeostasis of neuronal cells (Wright et al. 2012; Lun et al. 2015). Its potential to reflect changes in the CNS makes CSF one of the preferred sources to study early *in vivo* biomarkers in neurological pathologies (Lleó et al. 2015).

So far, potential biomarkers for human prion diseases have been studied in cerebrospinal fluid. These include direct detection of prion seeding activity, notably by means of the ultrasensitive technique real-time quaking-induced conversion (RT-QuIC), but also surrogate biomarkers of neuronal damage, among which we can highlight 14-3-3 and tau proteins for being commonly used in human clinical practice (Zerr 2022). However, these surrogate biomarkers are found to be dysregulated after neuronal damage and they are thus not highly specific for TSE. Besides, and more importantly, they can only be detected in an advanced stage of neurodegeneration, having low sensitivity in early stages of disease (Thompson and Mead 2019; Zerr 2022). Although some presymptomatic abnormalities have been reported using magnetic resonance imaging in a patient carrying a predisposing mutation for Creutzfeldt-Jakob disease (Koizumi et al. 2021), clinical diagnosis of these rapid progressive diseases is frequently made in the late stages, especially in non-predictable sporadic patients. Therefore, *in vivo* biomarkers to enable early diagnosis of prion diseases are urgently needed.

For this objective, proteomic analysis using mass spectrometry has been a breakthrough as one of the most powerful techniques for high-throughput identification and quantification of proteins. CSF proteomic approaches have already been conducted to search for biomarkers and gain a deeper understanding of the proteome function in neurodegenerative diseases (Pal et al. 2015; Puranik et al. 2020). Data-dependent acquisition (DDA) methods are still the most accurate for protein identification, while data-independent acquisition (DIA) ones are used for quantification. In the last years, the SWATH-MS (Sequential window acquisition of all theoretical mass spectra) technique has greatly contributed to the field of protein quantification as a variant of DIA methods, reducing interferences in ion detection and increasing the proteome coverage obtained by other techniques (Anjo et al. 2019; Chantada-Vázquez et al. 2021).

In this study, we aimed to discover new potential CSF biomarkers for prion diseases in the preclinical stage of sheep scrapie as a model of these disorders, combining the proteomic mass spectrometry approach with an ELISA (enzyme-like immunosorbent assay) validation of the most significantly dysregulated proteins. This combined technology could provide new insights into the early diagnosis of these diseases.

Materials and methods

Ethics statement

All experimental procedures in animals comply with the ARRIVE guidelines and have been conducted under the projects with references PI02/08 and PI21/13, approved by the Ethical Committee for Animal Experimentation of the University of Zaragoza. Animals were treated in accordance with the Spanish Royal Decree 53/2013, which complies with the European Directive 2010/63 on the protection of animals used for experimental and other scientific purposes.

Animals

A total of 30 Rasa Aragonesa female sheep were included in this study, with an average age of 4 years and 9 months and a standard deviation of 27 months. All of them were genotyped for *PRNP* polymorphisms, as previously reported (Acín et al. 2004), and displayed the ARQ/ARQ genotype, which is one of the most frequent genotypes in the scrapie-affected Rasa Aragonesa sheep (Acín et al. 2004). These animals were divided into three groups according to their scrapie-infection condition and stage of the disease: healthy controls, preclinical stage sheep and clinical stage sheep. The mean ages among the three groups were similar (one-way ANOVA-analysis of variance-test, *p*-value > 0.05). Healthy animals (*n* = 12) were selected from flocks located in areas where no scrapie cases had been reported. Scrapie-infected animals (*n* = 18) were obtained from several scrapie-affected flocks. From these, animals in the preclinical stage of the disease (*n* = 5) were identified before showing clinical signs by immunohistochemistry of rectal mucosa biopsy, as already described (González et al. 2008). Sheep in the clinical stage (*n* = 13) were identified by the observation of typical scrapie clinical signs, the most notable being pruritus with the appearance of alopecic areas around the lumbar region and tail, alteration of mental status, cachexia, ataxia, teeth grinding and head tremors (Vargas et al. 2005). The median time that the clinical scrapie-infected animals lived showing clinical signs was 1.6 months, with an interquartile range of 4 months. The prion infection in both groups of sheep was confirmed *post mortem* by immunohistochemical detection of PrP^Sc in the CNS, as previously described (Monleón et al. 2004).

Sample collection

Sheep were euthanised in the Centre for Encephalopathies and Emerging Transmissible Diseases at the University of Zaragoza by an intravenous injection of sodium pentobarbital and exsanguination, and the necropsy was performed right after. Three to five mL of CSF were collected into polypropylene tubes, immediately placed on ice and processed within one hour post extraction. After checking for no visible blood

contamination, CSF samples were aliquoted and preserved at −80 °C until used. One mL of CSF was sent to the Proteomic Unit at the Health Research Institute in Santiago de Compostela – IDIS, where the proteomic analyses were performed.

Protein in-gel digestion

Protein concentration was quantified using RC DC Protein Assay Kit (Bio-Rad, USA) according to the manufacturer's protocol and no depletion of most concentrated proteins was applied due to the lack of specific kits for sheep. An equal amount of protein of each sample was mixed with loading buffer, prepared with 10% SDS (sodium dodecyl sulphate), 500 mM DTT (dithiothreitol), 50% glycerol, 500 mM Tris-HCl and 0.05% bromophenol blue dye. The mix was then heated at 95 °C for 5 min and loaded into a 10% Tris-glycine SDS-polyacrylamide gel. It was submitted to 40V electrophoresis through the stacking gel, which was later upgraded to 80V. When the migration front was 3 mm into the resolving gel, electrophoresis was stopped, and the gel was stained with Coomassie staining. The gel was placed into a destaining solution containing 45% methanol and 7.5% acetic acid solution overnight. Next, the protein band of each sample was excised and subjected to an in-gel tryptic digestion, as described previously (Chantada-Vázquez et al. 2021). Briefly, gel pieces were washed, dehydrated, reduced with DTT (10 mM, in 50 mM ammonium bicarbonate) and alkylated with iodoacetamide (55 mM, in 50 mM ammonium bicarbonate). Later, modified porcine trypsin (Promega, USA) was added at a final concentration of 25 ng/μL trypsin in 20 mM ammonium bicarbonate, and digestion was left at 37 °C overnight. After digestion with trypsin, peptides were extracted from the gel using three incubations with a 60% acetonitrile and 0.5% formic acid solution. Finally, they were vacuum dried and kept at −20 °C until processed.

Protein identification by RPLC-MS/MS analysis

From each sample, 4 μg of digested peptides were diluted in 0.1% formic acid by sonication and loaded into a microflow liquid chromatography system (Eksigent Technologies nanoLC 400, Sciex, USA) coupled to a TripleTOF 6600 mass spectrometer (Sciex, USA), using a flow rate of 10 μL/min. First, samples went through a YMC-TRIART C18 200 × 0.05 mm precolumn (YMC Technologies, Teknokroma), with a 120 Å pore size and 3 μm particle size. The analytical column was a silica-based reverse phase Chrom XP C18 150 × 0.3 mm column (Eksigent, Sciex, USA), with same pore and particle sizes as the precolumn, where reverse phase liquid chromatography (RPLC) separation at a 5 μL/min flow rate took place. Mobile phase A was 0.1% formic acid in water, while mobile phase B was 0.1% formic acid in acetonitrile. Peptides were separated by RPLC using a 90-minute gradient ranging from 2% to 90% of mobile phase B and analysed on a TripleTOF 6600 QTOF (Quadrupole Time-Of-Flight) instrument using a DDA workflow, with the Analyst TF (version 1.7.1) software. Best interface conditions were previously determined and used (Chantada-Vázquez et al. 2020, 2021).

Library preparation and protein quantification by SWATH-MS analysis

All samples from each group were pooled and the three resulting pools were loaded into the microflow reverse phase liquid chromatography tandem mass spectrometry (microRPLC-MS/MS) for library preparation. The same procedure described above was performed using a DDA workflow, but using a 40-minute gradient on this occasion. All MS/MS spectra were obtained using the PeakView 2.2 software for the calculation of superposed variable windows with a SWATH-MS Variable Window Calculator (Sciex, USA). A hundred windows were created and imported into Analyst TF 1.7.1, the mass spectrometer software. Each sample was then loaded in duplicates into the same equipment but using a SWATH-MS acquisition method and previously described parameters (Chantada-Vázquez et al. 2020).

Bioinformatic data analysis

Peptide and protein identifications were performed using ProteinPilot 5.0.1 software (Sciex, USA) with a sheep specific (*Ovis aries*) Uniprot database. False discovery rate (FDR), which reflects an estimate of the chance an individual peptide or protein identification is incorrect, was set to 1%.

Furthermore, the data from the SWATH-MS method were analysed by PeakView 2.2 software using the SWATH Acquisition MicroApp (version 2.2) and based on the spectral library created with the DDA method, comprising a thousand proteins identified with a confidence score above 99%. Peptide retention time calibration was performed using peptides from the proteins identified in our samples. Protein peak areas were obtained by summing ten peptide peak areas per protein and seven ion fragment peak areas per peptide, and only peptides with FDR less than 1% were used for protein quantification. These peak areas were then exported to the MarkerView software for quantitative analysis and a global normalisation based on the total sum of all peak areas was done, thus controlling a possible uneven loss of sample during preparation. A Student's t test between groups was done for all possible comparisons, obtaining a p-value. Fold change (FC) was calculated as the ratio of the arithmetic mean of all samples in each group and presented as a base-2 logarithm ($\log_2$).

Unsupervised multivariate statistical analysis using principal component analysis (PCA) was conducted in R (version 4.2.2, ggfortify package) to compare

sample data across the three groups studied, using a logarithmic transformation of peak area data before the analysis. Heatmap was designed using the ComplexHeatmap version 2.14.0 R package. Fold changes of healthy samples were calculated by dividing the peak area of each healthy sheep by the mean of peak areas of all infected samples, whereas fold changes of preclinical and clinical sheep peak areas were referred to the mean of the healthy group. Z-score was calculated in R using the scale function and a heatmap was plotted. A complete linkage method and the Spearman Rank Correlation method for distance calculation were used for clustering proteins.

Venn diagrams and volcano plots were also designed to graph all proteomic data, using the VennDiagram and ggplot2 R packages, respectively.

Enrichment of KEGG (Kyoto Encyclopaedia of Genes and Genomes) pathways and GO (Gene Ontology) terms were examined using DAVID (Database for Annotation, Visualization and Integrated Discovery) (version Dec. 2021, accessible at https://david.ncifcrf.gov/) and ShinyGO (version 0.77, accessible at http://bioinformatics.sdstate.edu/go/) tools (Ge et al. 2020; Sherman et al. 2022). FunRich (version 3.1.3) was also used for functional enrichment analysis comparing proteins in the three groups studied. Protein interactions were examined with STRING (Search Tool for the Retrieval of Interacting Genes/Proteins) (version 11.5, accessible at https://string-db.org/), using a high confidence interaction score threshold of 0.7.

ELISA validation

Based on a comprehensive analysis of both DDA-MS and SWATH-MS results, we selected potential biomarkers for validation using the ELISA technique. We prioritised proteins that were significantly dysregulated in the preclinical group compared to healthy controls in the SWATH-MS analysis, while also considering proteins uniquely identified in the preclinical group by the DDA-MS method. This complementary approach allowed us to identify five proteins with strong potential as early-stage biomarkers. Proteins with their corresponding ELISA kits and dilution of CSF samples, indicated as ratio of CSF sample to diluent volume, are listed as follows: SYNCRIP (1:10, E14H0387, BlueGene, China), PLD3 (Undiluted, MBS9361401, MyBioSource, USA), C4 complement (1:4, E14C0012, BlueGene, China), SPP1 (1:250, E14O0005, BlueGene, China), CTSD (1:1, E14C0651, BlueGene, China). All samples were analysed in duplicate and the manufacturer's protocols were followed. Briefly, in PLD3 protocol, 50 μL of standards and samples were added to a 96-well plate. Right after, 100 μL of horseradish peroxidase conjugate reagent was added and the plate was incubated at 37 °C for one hour. After washing all the wells four times with wash solution, chromogen solutions A and B were added (50 μL from each) and the plate was incubated for 15 min at 37 °C protected from light. The reaction was stopped by adding 50 μL of stop solution and the optical density (OD) was measured at 450 nm immediately after, using an ELISA reader (Sunrise, Tecan). The protocol for the other four proteins varied slightly. A volume of 100 μL of each standard and sample was needed and 10 μL of a balance solution provided by each kit were mixed in each well. Next, 50 μL of conjugate were added and the same incubation and developing procedures were followed, reading the plate OD at 450 nm.

Statistical analysis

All statistical analyses were performed in R (version 4.2.2).

ELISA OD sample results were subtracted by the mean value of blank controls. Intra-assay coefficients of variation were calculated as a percentage ratio of the standard deviation to the mean of replicates OD, obtaining values in all cases below 10%. Inter-assay coefficients of variation were as well calculated with a subset of 10–15 samples per protein to check plate-to-plate variation, giving values below 15%. The standards data were plotted, and a third- or fourth-degree polynomial curve was fitted. Sample concentrations were determined by regression analysis.

Normal distribution of data was checked using a quantile-quantile plot (ggpubr R package) and the Shapiro-Wilk test (stats R package), recommended when having less than 50 samples. For normally distributed data, the homogeneity of variances was studied using Levene's test (car R package) for its lower sensitivity to departures from the normal distribution. When assuming normality and homogeneity of variance, the one-way ANOVA test (stats R package) was used for comparing the three groups analysed, followed by the Tukey HSD (Honestly-significant-difference) test (stats R package) for multiple pairwise-comparisons between the means of the groups. When the assumptions of normality and homogeneity of variance were not met, Kruskal-Wallis test (stats R package) was performed, followed by Dunn's test (FSA R package) for multiple pairwise-comparisons.

Continuous normally distributed variables were expressed as mean ± standard deviation, whereas non-normally distributed variables were summarised as median ± interquartile range. Box plots were designed using the ggplot2 R package.

Results

We analysed cerebrospinal fluid samples in two different stages of the classical scrapie infection in sheep, preclinical ($n = 5$) and clinical ($n = 13$) stages, and the results were compared with those obtained in healthy control animals ($n = 12$).

First, a qualitative analysis using microRPLC-MS/MS in a DDA mode was performed to identify the proteins expressed in the cerebrospinal fluid samples. In

all cases, only proteins with an FDR less than 0.01 were selected. Then, we did a complementary quantitative analysis using the SWATH-MS method to calculate protein expression differences between groups.

Several proteins are uniquely identified in scrapie-infected animals by qualitative analyses

Two different qualitative analyses were performed with the DDA data. We first selected the common proteins found in at least all but one samples per group ('*n − 1* analysis', being *n* the total number of samples per group), and a total of 222 proteins were identified. As shown in Figure 1A, we detected 27 unique proteins in the preclinical stage of the scrapie infection. Enrichment analyses of metabolic pathways using KEGG revealed that these proteins were associated with regulation of actin cytoskeleton and proteoglycans pathways. In addition, the five unique proteins identified in the clinical stage of the disease were mainly associated with the carbon metabolism pathway.

We then ran a second, less restrictive analysis and compared the results with those of the previous one. Considering that the non-detection of a protein in a sample may be due to a change in its polarity conditions causing it to become undetectable by mass analysis, rather than due to its absence, we took all common and uncommon proteins in all samples of each group (Figure 1B). In this case, a total of 1160 proteins were identified. Among these, 24 proteins were detected only in the preclinical stage, including proteins connected to oxygen transport, regarding a biological process analysis. Besides, on the metabolic pathway enrichment analyses performed using KEGG, protein digestion and absorption and oestrogen and insulin signalling pathways were associated with the 123 proteins uniquely identified in clinical scrapie sheep.

Proteins uniquely identified in preclinical and clinical stages of disease in both analyses are listed in Supplementary Table S1.

Functional enrichment analyses were performed on FunRich with all the proteins obtained from the second qualitative analysis detailed above (common and uncommon proteins). Figure 2 shows the percentage of proteins involved in ten biological processes at each stage of the infection. Briefly, the percentage of proteins associated with proteolysis and cell adhesion was found to be higher in scrapie-infected animals compared to healthy controls. A similar pattern was also observed for the immune system, complement activation and inflammatory response processes. On the other hand, proteins linked to protein folding and protein and ion transport processes were underrepresented in the preclinical stage of the disease.

Quantitative analyses identify significantly dysregulated proteins involved in neurodegeneration in preclinical stages

Quantitative analysis using the SWATH-MS method was performed to determine the significantly dysregulated expression of proteins in CSF between the preclinical and clinical stages of scrapie infection compared to healthy controls. To achieve this, we pooled all samples from each experimental group and used the pools to generate a library of a thousand proteins that was later used to reanalyse the samples using a SWATH-MS acquisition methodology.

First, a PCA was performed as an unsupervised method for reducing the dimensionality of our large dataset to compare samples across the groups. Principal component 1 explained 99.42% of the variance between samples (Supplementary Figure S1).

After the PCA, a comparison between scrapie-infected animals (clinical and preclinical) and healthy controls was performed. Significantly dysregulated proteins were considered those with a *p*-value less than 0.05 and an absolute value of $\log_2$FC higher than 0.5. In this comparison, 27 proteins were found to be upregulated in infected sheep (both preclinical and clinical) compared to healthy controls and
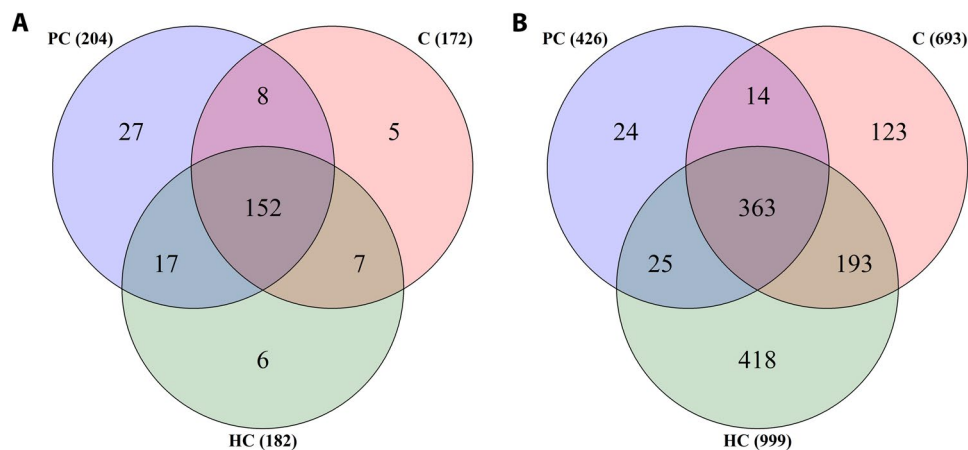

Figure 1. Venn diagrams showing the distribution of proteins among the two scrapie-infected groups studied in the preclinical stage (PC) and clinical stage (C), compared to the healthy control group (HC). The total number of proteins identified in each group is specified next to the group name. Proteins shown were identified by microRPLC-MS/MS using a DDA mode: A) in all but one samples (n − 1) per group; B) common and uncommon proteins in every sample of each group.

122 proteins were downregulated in infected animals compared to the control group (Supplementary Figure S2 and Table S2). We performed a GO analysis on the set of these 149 significantly dysregulated proteins. As shown in Figure 3, amino acid and carbon metabolism, complement cascades, oxidative phosphorylation and routes related to neurodegenerative diseases were among the most altered pathways.

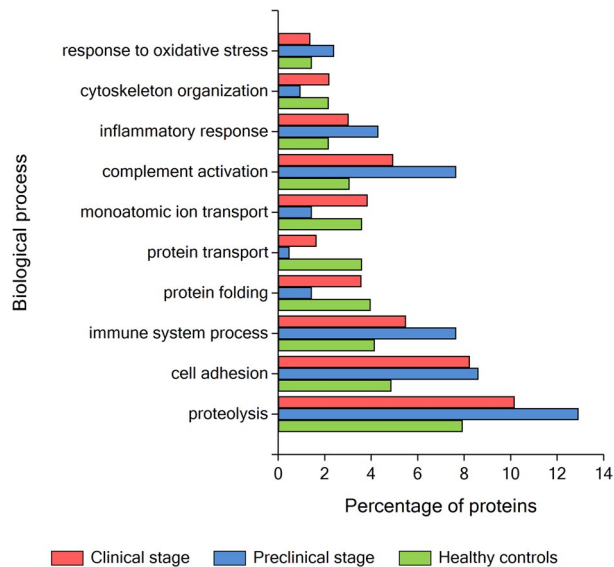Additional comparisons between groups were performed using volcano plots, looking for significantly dysregulated proteins with a more restrictive p-value < 0.01 and an absolute value of $\log_2FC > 0.5$. Specifically, and from this point onward, we focused on the preclinical stage versus healthy controls comparison, trying to elucidate potential biomarkers that change their expression in the earliest stage of the disease. A total of 33 proteins were significantly upregulated in the preclinical sheep compared to healthy sheep, whereas 13 proteins were significantly downregulated in the preclinical stage compared to the control group (Figure 4A and Table 1). On the other hand, regarding the clinical stage versus healthy group comparison, 110 proteins were significantly downregulated in clinical animals, whereas only 17 were upregulated in that same group (Figure 4B and Supplementary Table S3). Finally, we detected many more downregulated than upregulated proteins in the clinical stage compared to the preclinical one (Figure 4C and Supplementary Table S4).

Next, as shown in Figure 5, a heatmap analysis of the 46 preclinical-stage significantly dysregulated proteins was designed to graphically represent fold change values (converted into z-score values) of the peak areas of these proteins in all three groups of analysed animals (healthy, preclinical and clinical). Clustering analysis revealed two main clusters of proteins, one including proteins with lower expression in the infected individuals (both preclinical and clinical) than in the healthy control group, and another that contained proteins with higher expression in infected animals than in healthy ones.

Furthermore, we studied the potential interactions between these significantly preclinical-stage dysregulated proteins using the *Ovis aries* STRING database, as shown in Figure 6. Only 38 out of the total of 46 dysregulated proteins were in the STRING database and included in the network.

Figure 2. Functional enrichment analysis by FunRich performed on all proteins identified by the common and uncommon analysis of the DDA data. Bars represent the percentage of proteins assigned to each biological process, for each of the clinical stages.
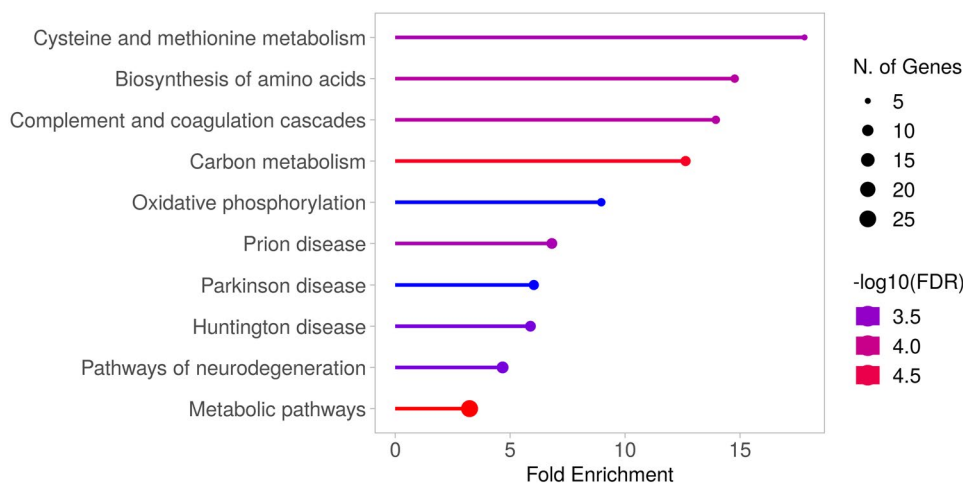

Figure 3. Gene Ontology analysis regarding KEGG pathways using ShinyGO, in which genes encoding significantly dysregulated proteins in the infected group compared to healthy animals with p-value < 0.05 and absolute value of $\log_2FC > 0.5$ are involved. Top 10 KEGG pathways altered are displayed, sorted by fold enrichment. Fold enrichment shows the ratio between the relative frequency of dysregulated proteins annotated to that pathway, and the total number of proteins in the reference species. Colour varies depending on the significance (-$\log_{10}$FDR), where the false discovery rate (FDR) value reflects the statistical chance of observing a number of proteins in a given list annotated to a specific pathway. Circle size shows the number of genes encoding input proteins involved in each pathway.

Another 20 proteins were also added by STRING considering their predicted functional similarities to the original set. The definitive network obtained had 58 proteins (nodes) and 60 interactions (edges), with a protein-protein interaction enrichment *p*-value of 3.31E-08. The most interesting biological processes involved were response to stress, cell adhesion and inflammatory response. Additionally, the molecular function of protein binding and KEGG pathways such as extracellular matrix receptor interaction and complement and coagulation cascades were identified as potentially related to neurodegenerative diseases.

Five proteins identified as potential diagnostic biomarkers in scrapie cerebrospinal fluid

Following an integrated evaluation of the DDA data and SWATH results, specifically in the comparison of the preclinical stage and healthy control groups, we chose five proteins to be validated in CSF samples by ELISA. SYNCRIP (Synaptotagmin binding, cytoplasmic RNA interacting protein) was the first selected, as it was identified both significantly upregulated in the SWATH analysis and uniquely identified in the preclinical group by DDA (Supplementary Figure S3). The other four proteins, PLD3 (Phospholipase D family member 3), C4 (Complement component 4), CTSD
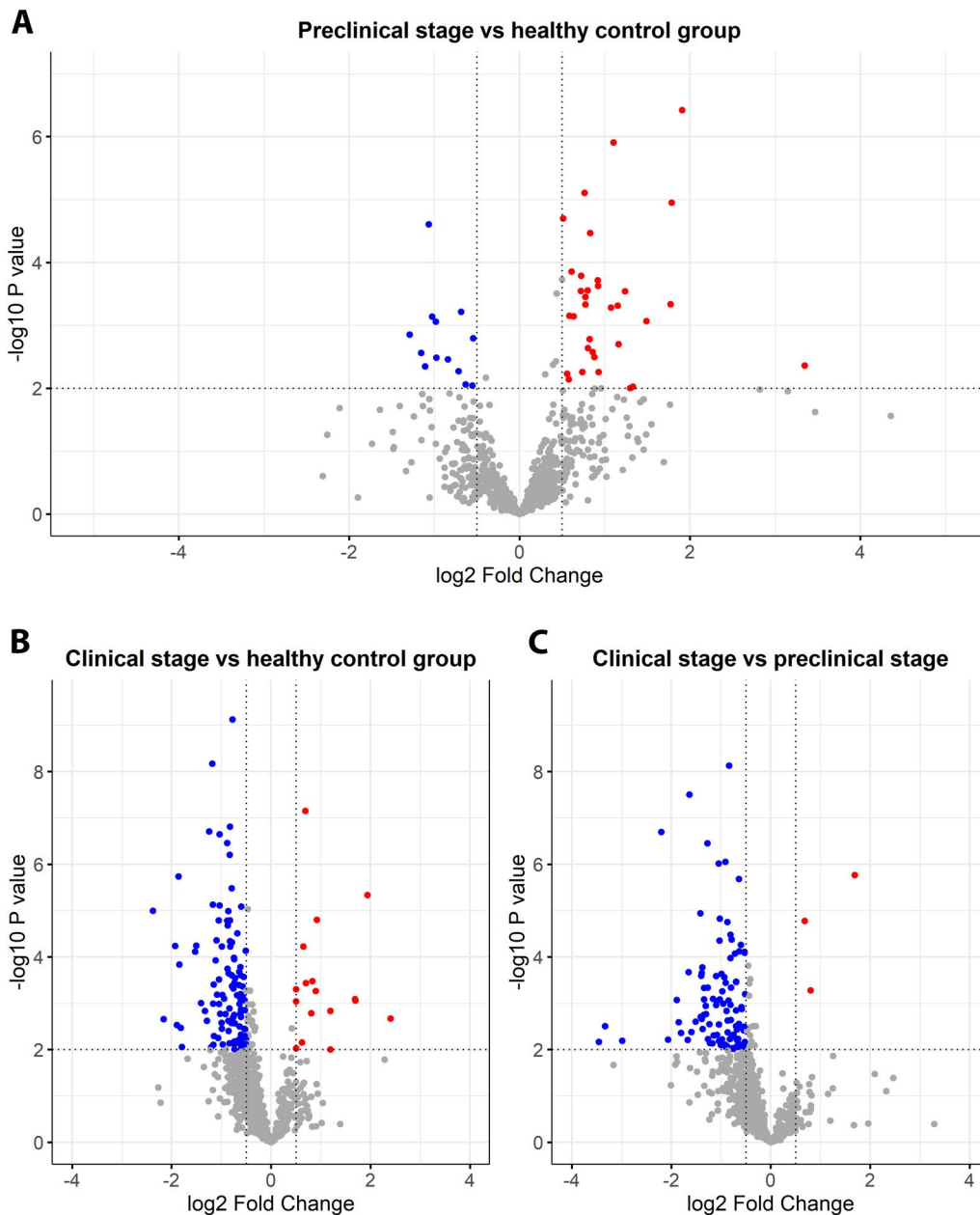

Figure 4. Volcano plots showing the results of the SWATH-MS analysis of CSF protein expression, representing three of the possible comparisons between groups: A) the preclinical stage group compared to the healthy control group; B) the clinical stage group compared to the healthy control group; C) the clinical stage group compared to the preclinical stage group. In all plots, the horizontal dotted line indicates a statistical significance (-Log$_{10}$ *p*-value) of 2, i.e. a *p*-value of 0.01, while the vertical dotted lines represent fold change values (Log$_2$ Fold Change) of −0.5 and +0.5, respectively. In each comparison, significantly upregulated CSF proteins are coloured in red and significantly downregulated CSF proteins are shown in blue. In grey, proteins without notable variation are marked.

Table 1. Significantly dysregulated proteins by SWATH-MS with *p*-value < 0.01 and absolute value of log$_2$FC > 0.5, upregulated (positive log$_2$FC, in green) and downregulated (negative log$_2$FC, in red) in the preclinical stage group, compared to the healthy control group.

UniProt code	Protein name	Gene name	*p*-value	Log$_2$FC
W5PUJ4	Synaptotagmin binding cytoplasmic RNA interacting protein	SYNCRIP	3.79E-07	1.9080
W5Q611	Keratin 1	KRT1	1.23E-06	1.1040
W5PV25	Chromogranin A	CHGA	7.82E-06	0.7627
W5P9G8	Phospholipase D family member 3	PLD3	1.12E-05	1.7877
W5PZI1	Clusterin	CLU	2.00E-05	0.5120
W5Q160	Keratin 10	KRT10	3.42E-05	0.8281
W5NSA6	Alpha-2-macroglobulin	A2M	1.39E-04	0.6101
G3LUQ4	Alpha-S1-casein	CSN1S1	1.63E-04	0.7229
W5Q9H2	Protein disulfide-isomerase	P4HB	1.93E-04	0.9196
W5P7W2	Stromal cell derived factor 4	SDF4	2.36E-04	0.9210
K4GWI0	2′,3′-cyclic-nucleotide 3′-phosphodiesterase	CNP	2.78E-04	0.8010
P12303	Transthyretin	TTR	2.84E-04	0.7207
W5P3V7	Myelin associated glycoprotein	MAG	2.87E-04	1.2398
W8TGE9	Thioredoxin	trxA	3.53E-04	0.7741
W5PKU1	Phospholysine phosphohistidine inorganic pyrophosphate phosphatase	LHPP	4.62E-04	1.7733
Q9TTU5	Major prion protein	PrP	4.67E-04	0.7745
W5PZY7	Ubiquitin-40S ribosomal protein S27a	RPS27A	4.88E-04	1.1526
W5PD45	Vesicle amine transport 1 like	VAT1L	5.20E-04	1.0725
K4P1S5	Peptidyl-prolyl cis-trans isomerase	PPIA	7.07E-04	0.5838
W5Q687	Keratin 5	KRT5	7.22E-04	0.6335
W5P0Q4	Haptoglobin	HP	8.55E-04	1.4903
W5Q349	Potassium channel tetramerization domain containing 12	KCTD12	1.65E-03	0.8219
W5QEC3	Methyltransferase like 3	METTL3	1.99E-03	1.1629
Q29439	Complement component C4 (Fragment)	C4	2.31E-03	0.8035
Q9MZS8	Cathepsin D (Fragment)	CTSD	2.66E-03	0.8585
W5NX56	Osteopontin	SPP1	3.20E-03	0.8784
Q1KYZ7	Beta-A globin chain	HBBA	4.34E-03	3.3458
W5PMH1	Glutathione synthetase	GSS	5.54E-03	0.7351
W5PMS1	Cartilage oligomeric matrix protein	COMP	5.54E-03	0.9293
W5PAT6	Agrin	AGRN	5.87E-03	0.5580
W5P2C6	Calsyntenin 3	CLSTN3	7.22E-03	0.5767
W5P3R8	Carboxypeptidase Q	CPQ	9.42E-03	1.3320
W5QHS2	Matrix Gla protein	MGP	9.95E-03	1.2977
W5PH95	Immunoglobulin heavy constant mu	IGHM	2.47E-05	−1.0651
W5PSQ7	Immunoglobulin lambda-1 light chain-like	IGL1	6.10E-04	−0.6858
A2P2I3	VH region (Fragment)	VH	7.23E-04	−1.0243
W5Q0L2	Serpin family A member 5	SERPINA5	8.76E-04	−0.9834
W5P8R0	Uncharacterized protein	NDUFA4	1.41E-03	−1.2904
W5NV16	Ig-like domain-containing protein	W5NV16_SHEEP	1.61E-03	−0.5445
W5Q039	Tubulin beta chain	TUBB3	2.73E-03	−1.1546
W5PJP2	Neurofilament light	NEFL	3.26E-03	−0.9773
W5P9V5	Polymeric immunoglobulin receptor	PIGR	3.48E-03	−0.8420
W5NR63	Protein S100	S100A4	4.49E-03	−1.1087
A2P2G8	VH region (Fragment)	VH	5.34E-03	−0.7139
W5PGR8	Ependymin related 1	EPDR1	8.71E-03	−0.6334
W5Q3K6	Protein C, inactivator of coagulation factors Va and VIIIa	PROC	9.11E-03	−0.5547

The unknown gene names are annotated with the UniProt code.

(Cathepsin D) and SPP1 (Osteopontin), were chosen for their promising significant upregulation in the preclinical animals compared to healthy controls in the SWATH-MS analysis.

Figure 7 shows the ELISA concentrations of the five selected proteins in CSF samples. We obtained very similar data compared to that from the mass spectrometry results, thus validating the proteomic analysis done in this study. The first protein studied, SYNCRIP, was found to be significantly upregulated in the preclinical (63.9 ± 1.13 ng/mL, *p*-value = 1.34E-5) and clinical (55.7 ± 0.30 ng/mL, *p*-value = 5.83E-4) stages of the scrapie disease compared to healthy sheep (32.4 ± 16.10 ng/mL). Regarding PLD3 expression, significantly higher concentrations were found in preclinical (6.29 ± 0.37 ng/mL, *p*-value = 3.62E-3) and clinical (6.01 ± 0.46 ng/mL, *p*-value = 5.93E-3) infected sheep compared to healthy controls (5.31 ± 0.61 ng/mL). Complement C4 concentration followed the same pattern, with a significantly upregulated expression in the preclinical (89.3 ± 16.3 ug/mL,

p-value = 0.02) and clinical (97.0 ± 19.9 ug/mL, *p*-value = 5.85E-4) stages, compared to that in healthy sheep (73.4 ± 10.5 ug/mL). The expression of cathepsin D in the CSF of preclinical sheep was significantly higher (2.62 ± 0.279 ng/mL, *p*-value = 2.6E-6) than in the healthy control group (1.40 ± 0.306 ng/mL), but expression in the clinical stage group (1.11 ± 0.427 ng/mL) was indistinguishable from that of healthy sheep. Osteopontin expression was significantly higher in preclinical (107 ± 1.04 ng/mL, *p*-value = 0.0282) and clinical (104 ± 15.1 ng/mL, *p*-value = 0.03) sheep compared to the healthy control group (83.2 ± 20.6 ng/mL).

Discussion

Classical sheep scrapie is a valuable preclinical model for studying human prion diseases (Llorens et al. 2018; Zetterberg et al. 2019; López-Pérez et al. 2020), and shares key biophysical and biochemical features with other neurodegenerative disorders commonly called prion-like disorders, such as Alzheimer's
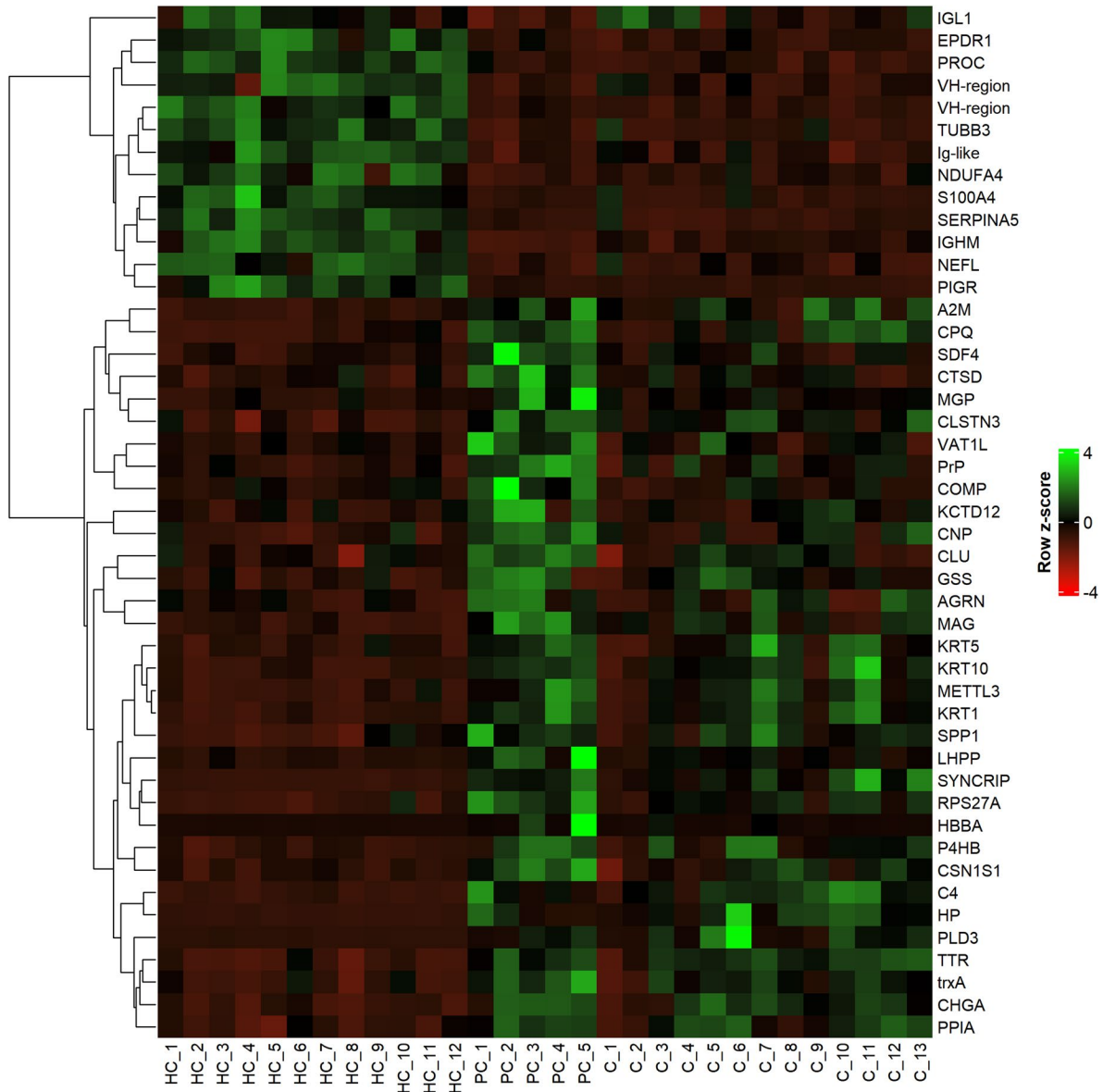
Figure 5. Heatmap analysis of the 46 significantly dysregulated proteins identified in the preclinical stage group and healthy group comparison. Relative expression of each protein is displayed with a colour range from red (downregulated) to green (upregulated), representing z-scores of the proteins' normalised peak areas. Clustering of proteins in rows, represented by a dendrogram in the left y-axis, was performed using a complete linkage method and the Spearman Rank Correlation method was applied for distance measurement. Columns represent all samples included in this study: 12 healthy sheep, 5 and 13 in the preclinical and clinical stages of the disease, respectively.

disease (AD) (Brundin et al. 2010; Frost and Diamond 2010). In the present study, we have performed for the first time the identification and quantification of the CSF proteome of naturally infected sheep with classical scrapie at two stages of the disease: a preclinical stage in which no clinical signs have yet appeared and on which we have mainly focused, and a clinical stage characterised by severe symptomatology close to a fatal outcome. Data from both stages have been compared with those of healthy animals to search for differences between groups. In the protein identification analysis, conducted by RPLC tandem mass spectrometry in DDA mode, we found remarkable qualitative differences in the proteome of the three groups, highlighting approximately twenty proteins that were only detected in preclinical animals. To further explore these

differences, we performed a quantitative analysis by SWATH-MS in which we identified 46 and 127 highly significant proteins differentially expressed in the preclinical and clinical stages of disease, respectively, compared to healthy controls. Among them, we selected five for validation by ELISA based on their significance and higher fold change in the preclinical stage and their functions and possible relationship with neurodegenerative diseases; these were SYNCRIP, PLD3, CTSD, C4 complement and SPP1.

It should be noted that a limited number of animals were used, specifically in the preclinical stage; this is due to the fact that we used naturally scrapie-affected animals, rather than experimentally infected ones, and that preclinical diagnosis of scrapie in sheep, although possible, can only provide a limited number of individuals. This may rise
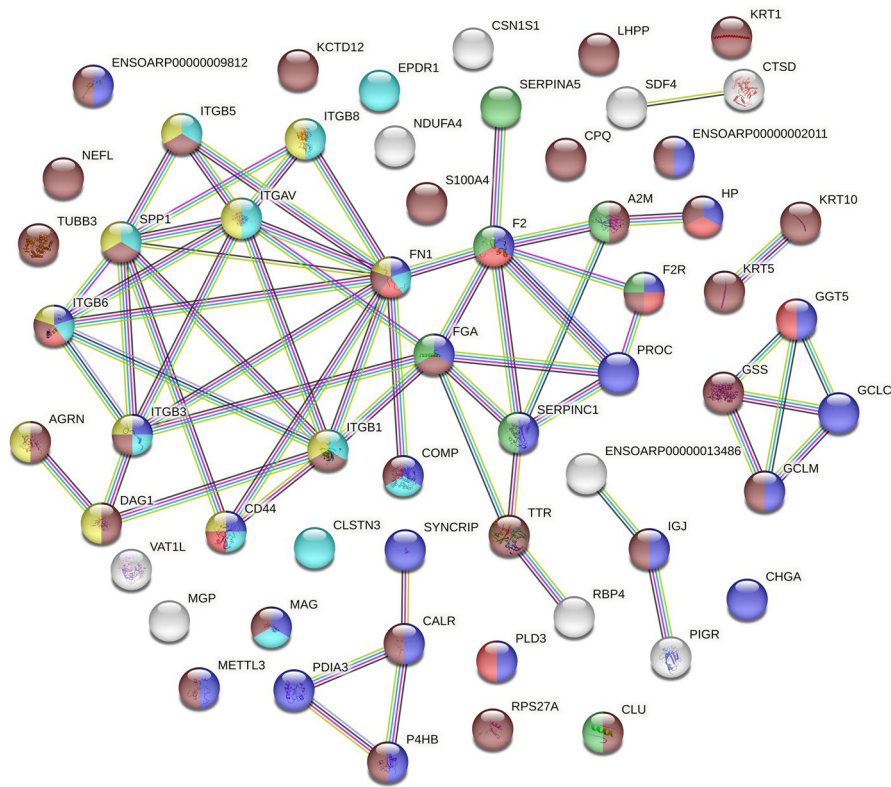
Figure 6. Interactions between proteins significantly dysregulated in the preclinical stage and those in the STRING sheep database. Network nodes (circles) represent individual proteins and edges refer to protein-protein association evidences, with a high confidence (0.700) interaction score. Edge (line) colours represent different interaction evidences: known interactions with light blue (from curated databases) and pink (experimentally determined), predicted co-occurrence with dark blue, text-mining with light green, co-expression with black and protein homology with purple. Node colours refer to functional enrichment analysis in which proteins are involved as follows: dark blue for response to stress, light blue for cell adhesion, red for inflammatory response, brown for protein binding, yellow for extracellular matrix receptor interaction and green for complement and coagulation Cascades.

questions about the statistical power of the differences observed in the preclinical group. Nevertheless, and even though they have to be interpreted cautiously, our results are promising and encourage further evaluation of these proteins as early biomarkers of prion diseases.

We have found numerous metabolic pathways altered by scrapie pathology. Among them, an increased inflammatory response was evidenced in clinical sheep compared to healthy sheep. It is well known that neuroinflammation is linked to neurodegenerative diseases, not only as a result of neurodegeneration but also potentially occurring before the accumulation of misfolded proteins (Kwon and Koh 2020; Zhang et al. 2023). Related to this, complement and coagulation cascades were also upregulated in infected animals when compared to healthy sheep; these same cascades have been found to be critical in synaptic plasticity and neuronal development in other brain-related disorders (Berkowitz et al. 2021; Heurich et al. 2022; Rydbirk et al. 2022). Additionally, in infected animals, we observed a disruption in proteins involved in amino acid and carbon metabolism pathways, which were also altered in metabolomic studies of CSF in AD patients, supporting the similarities between prion and other neurodegenerative diseases (Kaddurah-Daouk et al.

2013; Panyard et al. 2023). We have also detected altered oestrogen and insulin signalling pathways in clinical scrapie sheep. Both hormones have been previously studied for their function in brain development, and their dysregulation has been reported in AD and other neurodegenerative diseases (Zárate et al. 2017; Shaughness et al. 2020; Tao and Cheng 2023). Interestingly, we have identified oxidative stress response, cytoskeleton organisation and ion transport pathways already altered in the preclinical stage of scrapie. These pathways are known hallmarks of neurodegenerative diseases, and this finding supports the existence of measurable metabolic alterations prior to the emergence of clinical signs (Wilson et al. 2023). Moreover, proteins involved in some of these metabolic pathways have also been proposed as potential biomarkers of scrapie since they have been identified to be already altered in the preclinical stage of the disease (López-Pérez et al. 2020; Lozada Ortiz et al. 2023).

Regarding the functions of the validated proteins, first, synaptotagmin binding, cytoplasmic RNA interacting protein (SYNCRIP) is an RNA-binding protein, primarily involved in nucleic acid metabolism (Geuens et al. 2016). SYNCRIP also binds to synaptotagmins, synapse proteins related to calcium-dependent membrane trafficking (Mizutani et al. 2000; Yoshihara and
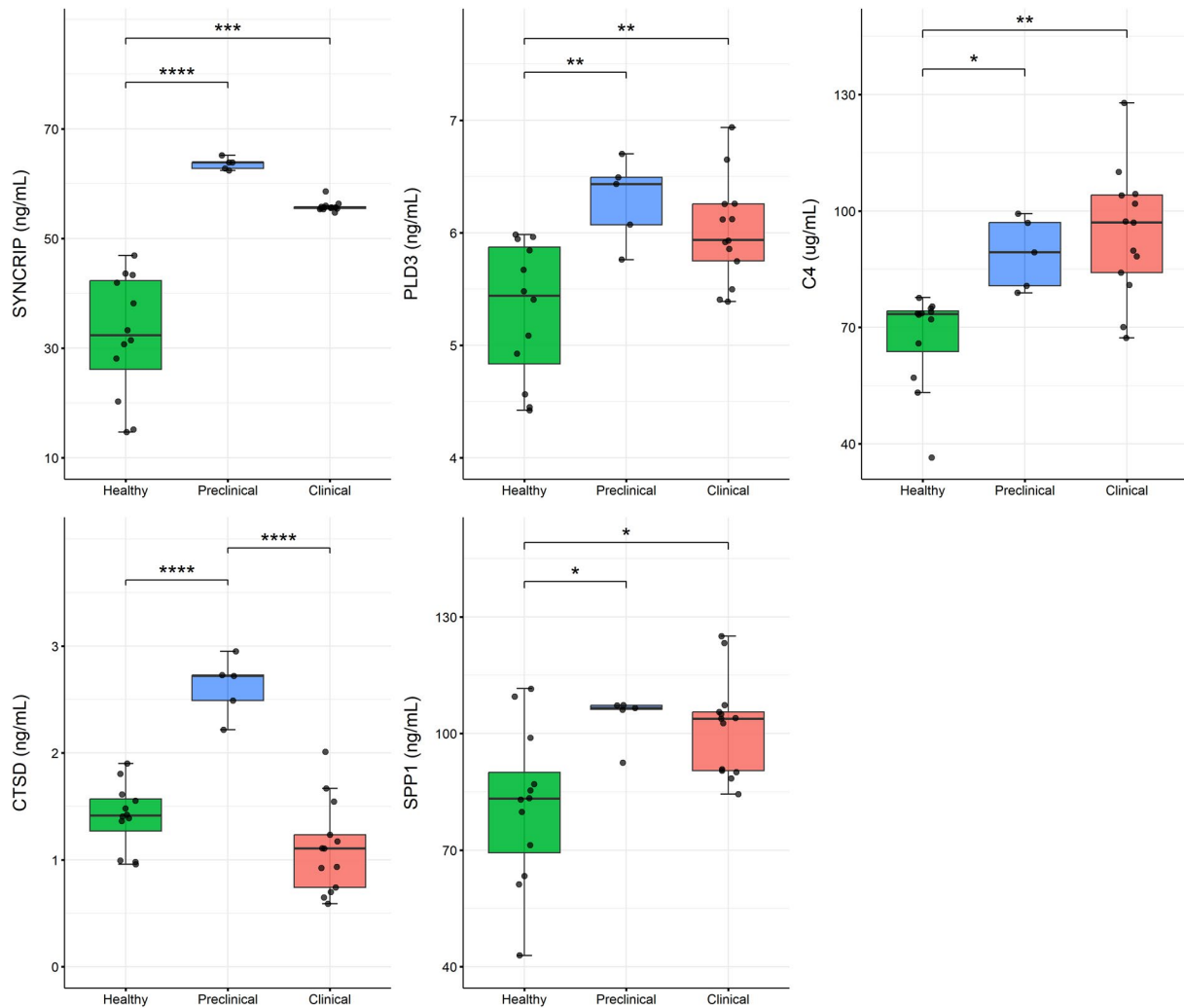
Figure 7. Concentration (Y-axis) of selected proteins (SYNCRIP, PLD3, C4, CTSD and SPP1) measured by ELISA in CSF samples of healthy controls ($n=12$) and preclinical ($n=5$) and clinical ($n=13$) scrapie-infected sheep. The boxes are drawn from the first quartile to the third quartile and the median is shown as a horizontal line inside the box. The whiskers extend from the box to the most extreme data point within 1.5 times the interquartile range, with the data points outside that range being considered potential outliers. Significant differences between groups were measured using one-way ANOVA test followed by Tukey HSD for multiple pairwise-comparisons or Kruskal-Wallis followed by Dunn's test, for normally and non-normally distributed data, respectively. *p-value < 0.05, **p-value < 0.01, ***p-value < 0.001, ****p-value < 0.0001.

Montana 2004), and calcium dysregulation can be the underlying cause of synaptic dysfunction and neuronal death in several neurodegenerative disorders (Zündorf and Reiser 2011). Besides, it has been related to the apolipoprotein B, a potential early marker of AD (Blanc et al. 2001; Picard et al. 2022). Furthermore, in our STRING interaction analysis, SYNCRIP had a strong interaction with calreticulin, a chaperone that prevents beta-amyloid aggregation (Reid et al. 2022). Few studies have been performed to detect SYNCRIP at the cellular and tissue levels, but no research has yet described its expression in CSF or any other accessible body fluid, and neither has it ever been studied in prion diseases. In the present study, we detected for the first time a highly significant increase in the expression of SYNCRIP in the CSF of preclinical and clinical scrapie-infected sheep, compared to that in healthy animals.

Besides, phospholipase D family member 3 (PLD3) is a neuronal lysosomal protein that has been associated with anti-apoptotic processes, neurotransmission

and neuronal survival (Pedersen et al. 1998; Wang et al. 2015; Gonzalez et al. 2018). Gene variants of this protein have been related to the risk of developing AD through beta-amyloid metabolism disruption (Cruchaga et al. 2014). Here we investigated this protein for the first time in a model of prion disease, reporting a significantly increased concentration of PLD3 in the CSF of infected animals, and already in the preclinical stage of the disease. This finding is supported by research showing that neuronal overexpression of PLD3 leads to an impairment of axonal conduction and neural network function (Yuan et al. 2022).

Like PLD3, cathepsin D (CTSD) is also localised in the lysosome, being a lysosomal aspartic protease with a variety of functions, such as protein degradation, antigen processing and presentation and regulation of apoptosis (Benes et al. 2008; Stoka et al. 2016). In our STRING analysis, CTSD had a close interaction with a calcium-binding protein. Besides, we found a significant increase of CTSD in the CSF of

preclinical sheep, while the concentration of this protein returned to basal levels in the clinical stage. Previous research supports our results since CTSD has already been found to be increased in the brain and CSF of AD patients (Schwagerl et al. 1995; Chai et al. 2019). Similarly, the CTSD gene has also been found to be upregulated in scrapie-infected mice and clinical sCJD brains (Diedrich et al. 1991; Xiang et al. 2004; Kovács et al. 2007; Llorens et al. 2017; Kanata et al. 2019).

Moreover, C4 complement is a key element in the classical innate immune system, controlling synaptic refinement to maintain optimal brain function and development, besides its contribution to the inflammation cascade (Rapino et al. 2023). Here, we have identified an increase in the concentration of C4 in CSF throughout the natural prion disease progression, as early as the preclinical stage in sheep. Most studies are in line with these results, with an increase of this protein being also reported in CSF from individuals affected by other neurodegenerative diseases, such as AD and multiple sclerosis (Wijte et al. 2012; Zelek et al. 2020). More recently, a significant increase of C4 protein levels in the CNS of sCJD patients has been described, as well as a remarkable overexpression at the gene level in a mouse model of sCJD in the preclinical stage (Llorens et al. 2014), in agreement with our own results.

Finally, osteopontin (SPP1) is an extracellular matrix phosphoprotein involved in inflammatory processes, acting as a cell adhesion molecule and as a proinflammatory cytokine (Lund et al. 2009; Rittling and Singh 2015; Stampanoni Bassi et al. 2023). The STRING analysis revealed its interaction with integrins and cell adhesion molecules, involved in inflammation processes and neurodegenerative diseases (Mezu-Ndubuisi and Maheshwari 2021; Shu et al. 2022). Here, we studied for the first time its expression in CSF in a natural model of prion disease and we found a significant increase in both the preclinical and clinical stages. This is consistent with numerous other studies conducted on SPP1, which found it to be increased in the CSF of AD (Comi et al. 2010; Sun et al. 2013) and the brain of CJD patients (Kanata et al. 2019; Cheng et al. 2023).

Although clarifying the reason for the observed changes in the CSF levels of these proteins is out of the scope of this study, we can hypothesise that their upregulation could be due to their delivery from the CNS (following neuronal death), excessive accumulation, or pathologically increased synthesis. Another related, unresolved question is whether the observed changes in protein levels predate the neurodegenerative process or else are their consequence. In this line, for example, it appears that the upregulation of SYNCRIP has a protective role in suppressing huntingtin protein aggregation in human neuroblastoma cells (Ryu et al. 2019), and in SYNCRIP-silenced cells, proinflammatory proteins expressed in the CNS are upregulated (Cappelli et al. 2018). Additionally, CTSD has been proved to degrade beta-amyloid and tau aggregates (Wang

et al. 2020; Gallwitz et al. 2022). Similarly, a recent study proposed that SPP1 has a promising role in beta-amyloid clearance and might act as a neuroprotective molecule in AD patients (Rentsendorj et al. 2018). All these observations lead to the interpretation of the upregulation of these proteins as a neuronal adaptive mechanism against protein aggregation. The reasons for the decrease in CTSD in clinical animals compared to the preclinical stage are unknown; it is perhaps due to the large accumulation of misfolded protein and the saturation of the apoptotic system in the terminal stage of disease, but further studies would be needed to verify this hypothesis.

In contrast, it is known that complement overactivation triggers early synaptic loss, which is associated with cognitive impairment in AD and other neurodegenerative diseases (Hong et al. 2016; Wu et al. 2019); thus, C4 upregulation could be understood as a cause rather than a consequence of the neurodegenerative process, although studies would be required to corroborate this hypothesis.

Overall, the present study provides, for the first time, insights on the CSF proteome of animals naturally infected with scrapie during the preclinical and clinical stages of the disease and contributes a battery of new and promising potential biomarkers validated in an *in vivo* model of natural prion disease. Although the results for the preclinical animals should be interpreted cautiously, further analyses are being performed to validate the results presented here and to elucidate and better understand the functions and roles of these differentially expressed proteins in the pathogenesis of neurodegenerative diseases.

Author contributions

All authors have read the journal's authorship agreement, reviewing and approving the final version of the present manuscript, and agreeing to be accountable for all aspects of this work. The co-author contributions according to the CRediT author contribution statement are as follows: conceptualization, T.B., J.R.R., J.J.B. and R.B.; methodology, S.P.-L., T.B., S.B.B. and I.M.-B.; software, S.P.-L., S.B.B. and M.d.P.C.-V.; formal analysis, S.P.-L., S.B.B. and I.M.-B.; investigation, S.P.-L., T.B., S.B.B. and M.d.P.C.-V.; writing – original draft, S.P.-L. and T.B.; writing – review and editing, T.B., S.B.B., E.S., A.O., I.M.-B., J.R.R., J.J.B. and R.B.; supervision, E.S., I.M.-B., J.R.R., J.J.B. and R.B. and funding acquisition, A.O., I.M.-B., J.J.B. and R.B.

Disclosure statement

No potential competing interest was reported by the authors.

Funding

Data availability statement

The mass spectrometry proteomics data have been deposited to the ProteomeXchange Consortium *via* the PRIDE partner repository with the dataset identifier PXD050656.

For the peer review process, please find below the reviewer account details to access the currently private dataset, until publication:

Username: reviewer_pxd050656@ebi.ac.uk
Password: JvrK2jAV

References

Acín C, Martín-Burriel I, Goldmann W, Lyahyai J, Monzón M, Bolea R, Smith A, Rodellar C, Badiola JJ, Zaragoza P. 2004. Prion protein gene polymorphisms in healthy and scrapie-affected Spanish sheep. J Gen Virol. 85(Pt 7):2103–2110. doi: 10.1099/vir.0.80047-0.

Anjo, S.I., Santa, C., Manadas, B. 2019. SWATH Mass Spectrometry applied to cerebrospinal fluid differential proteomics: establishment of a sample-specific method. In: Santamaría E, Fernández-Irigoyen J, editors. Cerebrospinal fluid (CSF) proteomics. Methods and protocols. Springer: Methods in Molecular Biology; p. 169–189. doi: 10.1007/978-1-4939-9706-0_11.

Benes P, Vetvicka V, Fusek M. 2008. Cathepsin D – many functions of one aspartic protease. Crit Rev Oncol Hematol. 68(1):12–28. doi: 10.1016/j.critrevonc.2008.02.008.

Berkowitz S, Chapman J, Dori A, Gofrit SG, Maggio N, Shavit-Stein E. 2021. Complement and coagulation system crosstalk in synaptic and neural conduction in the central and peripheral nervous systems. Biomedicines. 9(12):1950. doi: 10.3390/biomedicines9121950.

Blanc V, Navaratnam N, Henderson JO, Anant S, Kennedy S, Jarmuz A, Scott J, Davidson NO. 2001. Identification of GRY-RBP as an apolipoprotein B RNA-binding protein that interacts with both apobec-1 and apobec-1 complementation factor to modulate C to U editing. J Biol Chem. 276(13):10272–10283. doi: 10.1074/jbc.M006435200.

Brundin P, Melki R, Kopito R. 2010. Prion-like transmission of protein aggregates in neurodegenerative diseases. Nat Rev Mol Cell Biol. 11(4):301–307. doi: 10.1038/nrm2873.

Cappelli S, Romano M, Buratti E. 2018. Systematic analysis of gene expression profiles controlled by hnRNP Q and hnRNP R, two closely related human RNA binding proteins implicated in mRNA processing mechanisms. Front Mol Biosci. 5:79. doi: 10.3389/fmolb.2018.00079.

Chai YL, Chong JR, Weng J, Howlett D, Halsey A, Lee JH, Attems J, Aarsland D, Francis PT, Chen CP, et al. 2019. Lysosomal cathepsin D is upregulated in Alzheimer's disease neocortex and may be a marker for neurofibrillary degeneration. Brain Pathol. 29(1):63–74. doi: 10.1111/bpa.12631.

Chantada-Vázquez MP, Castro López A, García Vence M, Vázquez-Estévez S, Acea-Nebril B, Calatayud DG, Jardiel T, Bravo SB, Núñez C. 2020. Proteomic investigation on bio-corona of Au, Ag and Fe nanoparticles for the discovery of triple negative breast cancer serum protein biomarkers. J Proteomics. 212:103581. doi: 10.1016/j.jprot.2019.103581.

Chantada-Vázquez MP, García Vence M, Serna A, Núñez C, Bravo SB. 2021. SWATH-MS protocols in human diseases. In: Carrera M, Mateos J, editors. Shotgun proteomics. Methods and protocols. Springer: Methods in Molecular Biology; p. 105–141. doi: 10.1007/978-1-0716-1178-4_7.

Cheng Y, Chen T, Hu J. 2023. Genetic analysis of potential biomarkers and therapeutic targets in neuroinflammation from sporadic Creutzfeldt-Jakob disease. Sci Rep. 13(1):14122. doi: 10.1038/s41598-023-41066-9.

Comi C, Carecchio M, Chiocchetti A, Nicola S, Galimberti D, Fenoglio C, Cappellano G, Monaco F, Scarpini E, Dianzani U. 2010. Osteopontin is increased in the cerebrospinal fluid of patients with Alzheimer's disease and its levels correlate with cognitive decline. J Alzheimers Dis. 19(4):1143–1148. doi: 10.3233/JAD-2010-1309.

Cruchaga C, Karch CM, Jin SC, Benitez BA, Cai Y, Guerreiro R, Harari O, Norton J, Budde J, Bertelsen S, et al. 2014. Rare coding variants in the phospholipase D3 gene confer risk for Alzheimer's disease. Nature. 505(7484):550–554. doi: 10.1038/nature12825.

Diedrich JF, Minnigan H, Carp RI, Whitaker JN, Race R, Frey W, II, Haase AT. 1991. Neuropathological changes in scrapie and Alzheimer's disease are associated with increased expression of apolipoprotein E and cathepsin D in astrocytes. J Virol. 65(9):4759–4768. doi: 10.1128/JVI.65.9.4759-4768.1991.

Frost B, Diamond MI. 2010. Prion-like mechanisms in neurodegenerative diseases. Nat Rev Neurosci. 11(3):155–159. doi: 10.1038/nrn2786.

Gallwitz L, Schmidt L, Marques ARA, Tholey A, Cassidy L, Ulku I, Multhaup G, Di Spiezio A, Saftig P. 2022. Cathepsin D: analysis of its potential role as an amyloid beta degrading protease. Neurobiol Dis. 175:105919. doi: 10.1016/j.nbd.2022.105919.

Ge SX, Jung D, Yao R. 2020. ShinyGO: a graphical gene-set enrichment tool for animals and plants. Bioinformatics. 36(8):2628–2629. doi: 10.1093/bioinformatics/btz931.

Geuens T, Bouhy D, Timmerman V. 2016. The hnRNP family: insights into their role in health and disease. Hum Genet. 135(8):851–867. doi: 10.1007/s00439-016-1683-5.

Gonzalez AC, Schweizer M, Jagdmann S, Bernreuther C, Reinheckel T, Saftig P, Damme M. 2018. Unconventional trafficking of mammalian phospholipase D3 to lysosomes. Cell Rep. 22(4):1040–1053. doi: 10.1016/j.celrep.2017.12.100.

González L, Dagleish MP, Martin S, Dexter G, Steele P, Finlayson J, Jeffrey M. 2008. Diagnosis of preclinical scrapie in live sheep by the immunohistochemical examination of rectal biopsies. Vet Rec. 162(13):397–403. doi: 10.1136/vr.162.13.397.

Heurich M, Föcking M, Mongan D, Cagney G, Cotter DR. 2022. Dysregulation of complement and coagulation pathways: emerging mechanisms in the development of psychosis. Mol Psychiatry. 27(1):127–140. doi: 10.1038/s41380-021-01197-9.

Hong S, Beja-Glasser VF, Nfonoyim BM, Frouin A, Li S, Ramakrishnan S, Merry KM, Shi Q, Rosenthal A, Barres BA, et al. 2016. Complement and microglia mediate early synapse loss in Alzheimer mouse models. Science. 352(6286):712–716. doi: 10.1126/science.aad8373.

Kaddurah-Daouk R, Zhu H, Sharma S, Bogdanov M, Rozen SG, Matson W, Oki NO, Motsinger-Reif AA, Churchill E, Lei Z, et al. 2013. Alterations in metabolic pathways and networks in Alzheimer's disease. Transl Psychiatry. 3(4):e244–e244. doi: 10.1038/tp.2013.18.

Kanata E, Llorens F, Dafou D, Dimitriadis A, Thüne K, Xanthopoulos K, Bekas N, Espinosa JC, Schmitz M, Marín-Moreno A, et al. 2019. RNA editing alterations define manifestation of prion diseases. Proc Natl Acad Sci U S A. 116(39):19727–19735. doi: 10.1073/pnas.1803521116.

Koizumi R, Ueda N, Mugita A, Kimura K, Kishida H, Tanaka F. 2021. Case Report: extremely early detection of preclinical magnetic resonance imaging abnormality in

Creutzfeldt-Jakob disease with the V180I mutation. Front Neurol. 12:751750. doi: 10.3389/fneur.2021.751750.

Kovács GG, Gelpi E, Ströbel T, Ricken G, Nyengaard JR, Bernheimer H, Budka H. 2007. Involvement of the endosomal-lysosomal system correlates with regional pathology in Creutzfeldt-Jakob disease. J Neuropathol Exp Neurol. 66(7):628–636. doi: 10.1097/nen.0b013e318093ecc7.

Kwon HS, Koh SH. 2020. Neuroinflammation in neurodegenerative disorders: the roles of microglia and astrocytes. Transl Neurodegener. 9(1):42. doi: 10.1186/s40035-020-00221-2.

Lleó A, Cavedo E, Parnetti L, Vanderstichele H, Herukka SK, Andreasen N, Ghidoni R, Lewczuk P, Jeromin A, Winblad B, et al. 2015. Cerebrospinal fluid biomarkers in trials for Alzheimer and Parkinson diseases. Nat Rev Neurol. 11(1):41–55. doi: 10.1038/nrneurol.2014.232.

Llorens F, Barrio T, Correia Â, Villar-Piqué A, Thüne K, Lange P, Badiola JJ, Schmitz M, Lachmann I, Bolea R, et al. 2018. Cerebrospinal fluid prion disease biomarkers in pre-clinical and clinical naturally occurring scrapie. Mol Neurobiol. 55(11):8586–8591., doi: 10.1007/s12035-018-1014-z.

Llorens F, López-González I, Thüne K, Carmona M, Zafar S, Andréoletti O, Zerr I, Ferrer I. 2014. Subtype and regional-specific neuroinflammation in sporadic Creutzfeldt-Jakob disease. Front Aging Neurosci. 6:198. doi: 10.3389/fnagi.2014.00198.

Llorens F, Thüne K, Sikorska B, Schmitz M, Tahir W, Fernández-Borges N, Cramm M, Gotzmann N, Carmona M, Streichenberger N, et al. 2017. Altered Ca(2+) homeostasis induces Calpain-Cathepsin axis activation in sporadic Creutzfeldt-Jakob disease. Acta Neuropathol Commun. 5(1):35. doi: 10.1186/s40478-017-0431-y.

López-Pérez O, Bernal-Martín M, Hernaiz A, Llorens F, Betancor M, Otero A, Toivonen JM, Zaragoza P, Zerr I, Badiola JJ, et al. 2020. BAMBI and CHGA in prion diseases: neuropathological assessment and potential role as disease biomarkers. Biomolecules. 10(5):706. doi: 10.3390/biom10050706.

Lozada Ortiz J, Betancor M, Pérez Lázaro S, Bolea R, Badiola JJ, Otero A. 2023. Endoplasmic reticulum stress and ubiquitin-proteasome system impairment in natural scrapie. Front Mol Neurosci. 16:1175364. doi: 10.3389/fnmol.2023.1175364.

Lun MP, Monuki ES, Lehtinen MK. 2015. Development and functions of the choroid plexus-cerebrospinal fluid system. Nat Rev Neurosci. 16(8):445–457. doi: 10.1038/nrn3921.

Lund SA, Giachelli CM, Scatena M. 2009. The role of osteopontin in inflammatory processes. J Cell Commun Signal. 3(3-4):311–322. doi: 10.1007/s12079-009-0068-0.

Mackenzie G, Will R. 2017. Creutzfeldt-Jakob disease: recent developments. F1000Res. 6:2053. doi: 10.12688/f1000research.12681.1.

McGowan J. 1922. Scrapie in sheep. Scottish J Agric. 5:365–375.

Mezu-Ndubuisi OJ, Maheshwari A. 2021. The role of integrins in inflammation and angiogenesis. Pediatr Res. 89(7):1619–1626. doi: 10.1038/s41390-020-01177-9.

Mizutani A, Fukuda M, Ibata K, Shiraishi Y, Mikoshiba K. 2000. SYNCRIP, a cytoplasmic counterpart of heterogeneous nuclear ribonucleoprotein R, interacts with ubiquitous synaptotagmin isoforms. J Biol Chem. 275(13):9823–9831. doi: 10.1074/jbc.275.13.9823.

Monleón E, Garza MC, Sarasa R, Alvarez-Rodriguez J, Bolea R, Monzón M, Vargas MA, Badiola JJ, Acín C. 2011. An assessment of the efficiency of PrPSc detection in rectal mucosa and third-eyelid biopsies from animals infected with scrapie. Vet Microbiol. 147(3-4):237–243., doi: 10.1016/j.vetmic.2010.06.028.

Monleón E, Monzón M, Hortells P, Vargas A, Acín C, Badiola JJ. 2004. Detection of PrPSc on lymphoid tissues from naturally affected scrapie animals: comparison of three visualization systems. J Histochem Cytochem. 52(2):145–151. doi: 10.1177/002215540405200201.

Pal R, Larsen JP, Moller SG. 2015. The potential of proteomics in understanding neurodegeneration. Int Rev Neurobiol. 121:25–58. doi: 10.1016/bs.irn.2015.05.002.

Panyard DJ, McKetney J, Deming YK, Morrow AR, Ennis GE, Jonaitis EM, Van Hulle CA, Yang C, Sung YJ, Ali M, et al. 2023. Large-scale proteome and metabolome analysis of CSF implicates altered glucose and carbon metabolism and succinylcarnitine in Alzheimer's disease. Alzheimers Dement. 19(12):5447–5470. doi: 10.1002/alz.13130.

Pedersen KM, Finsen B, Celis JE, Jensen NA. 1998. Expression of a novel murine phospholipase D homolog coincides with late neuronal development in the forebrain. J Biol Chem. 273(47):31494–31504. doi: 10.1074/jbc.273.47.31494.

Picard C, Nilsson N, Labonté A, Auld D, Rosa-Neto P, Initiative A, Ashton NJ, Zetterberg H, Blennow K, Breitner JCB, et al. 2022. Apolipoprotein B is a novel marker for early tau pathology in Alzheimer's disease. Alzheimers Dement. 18(5):875–887. doi: 10.1002/alz.12442.

Prusiner SB. 1982. Novel proteinaceous infectious particles cause scrapie. Science. 216(4542):136–144. doi: 10.1126/science.6801762.

Puranik N, Yadav D, Yadav SK, Chavda VK, Jin JO. 2020. Proteomics and neurodegenerative disorders: advancements in the diagnostic analysis. Curr Protein Pept Sci. 21(12):1174–1183. doi: 10.2174/1389203721666200511094222.

Rapino F, Natoli T, Limone F, O'Connor E, Blank J, Tegtmeyer M, Chen W, Norabuena E, Narula J, Hazelbaker D, et al. 2023. Small-molecule screen reveals pathways that regulate C4 secretion in stem cell-derived astrocytes. Stem Cell Reports. 18(1):237–253. doi: 10.1016/j.stemcr.2022.11.018.

Reid KM, Kitchener EJA, Butler CA, Cockram TOJ, Brown GC. 2022. Brain cells release calreticulin that attracts and activates microglia, and inhibits amyloid beta aggregation and neurotoxicity. Front Immunol. 13:859686. doi: 10.3389/fimmu.2022.859686.

Rentsendorj A, Sheyn J, Fuchs DT, Daley D, Salumbides BC, Schubloom HE, Hart NJ, Li S, Hayden EY, Teplow DB, et al. 2018. A novel role for osteopontin in macrophage-mediated amyloid-beta clearance in Alzheimer's models. Brain Behav Immun. 67:163–180. doi: 10.1016/j.bbi.2017.08.019.

Rittling SR, Singh R. 2015. Osteopontin in immune-mediated diseases. J Dent Res. 94(12):1638–1645. doi: 10.1177/0022034515605270.

Rydbirk R, Østergaard O, Folke J, Hempel C, DellaValle B, Andresen TL, Løkkegaard A, Hejl AM, Bode M, Blaabjerg M, et al. 2022. Brain proteome profiling implicates the complement and coagulation cascade in multiple system atrophy brain pathology. Cell Mol Life Sci. 79(6):336. doi: 10.1007/s00018-022-04378-z.

Ryu HG, Kim S, Lee S, Lee E, Kim HJ, Kim DY, Kim KT. 2019. HNRNP Q suppresses polyglutamine huntingtin aggregation by post-transcriptional regulation of Vaccinia-related kinase 2. J Neurochem. 149(3):413–426. doi: 10.1111/jnc.14638.

Schwagerl AL, Mohan PS, Cataldo AM, Vonsattel JP, Kowall NW, Nixon RA. 1995. Elevated levels of the endosomal-lysosomal proteinase cathepsin D in cerebrospinal fluid in Alzheimer disease. J Neurochem. 64(1):443–446., doi: 10.1046/j.1471-4159.1995.64010443.x.

Shaughness M, Acs D, Brabazon F, Hockenbury N, Byrnes KR. 2020. Role of insulin in neurotrauma and neurodegeneration: a review. Front Neurosci. 14:547175. doi: 10.3389/fnins.2020.547175.

Sherman BT, Hao M, Qiu J, Jiao X, Baseler MW, Lane HC, Imamichi T, Chang W. 2022. DAVID: a web server for functional enrichment analysis and functional annotation of gene lists (2021 update). Nucleic Acids Res. 50(W1):W216–W221. doi: 10.1093/nar/gkac194.

Shu J, Li N, Wei W, Zhang L. 2022. Detection of molecular signatures and pathways shared by Alzheimer's disease and type 2 diabetes. Gene. 810:146070. doi: 10.1016/j.gene.2021.146070.

Stampanoni Bassi M, Buttari F, Gilio L, Iezzi E, Galifi G, Carbone F, Micillo T, Dolcetti E, Azzolini F, Bruno A, et al. 2023. Osteopontin is associated with multiple sclerosis relapses. Biomedicines. 11(1):178. doi: 10.3390/biomedicines11010178.

Stoka V, Turk V, Turk B. 2016. Lysosomal cathepsins and their regulation in aging and neurodegeneration. Ageing Res Rev. 32:22–37. doi: 10.1016/j.arr.2016.04.010.

Sun Y, Yin XS, Guo H, Han RK, He RD, Chi LJ. 2013. Elevated osteopontin levels in mild cognitive impairment and Alzheimer's disease. Mediators Inflamm. 2013:615745–615749. doi: 10.1155/2013/615745.

Tao Z, Cheng Z. 2023. Hormonal regulation of metabolism-recent lessons learned from insulin and estrogen. Clin Sci (Lond). 137(6):415–434. doi: 10.1042/CS20210519.

Thompson AGB, Mead SH. 2019. Review: fluid biomarkers in the human prion diseases. Mol Cell Neurosci. 97:81–92. doi: 10.1016/j.mcn.2018.12.003.

Vargas F, Bolea R, Monleón E, Acín C, Vargas A, De Blas I, Luján L, Badiola JJ. 2005. Clinical characterisation of natural scrapie in a native Spanish breed of sheep. Vet Rec. 156(10):318–320., doi: 10.1136/vr.156.10.318.

Wang Y, Wu Q, Anand BG, Karthivashan G, Phukan G, Yang J, Thinakaran G, Westaway D, Kar S. 2020. Significance of cytosolic cathepsin D in Alzheimer's disease pathology: protective cellular effects of PLGA nanoparticles against beta-amyloid-toxicity. Neuropathol Appl Neurobiol. 46(7):686–706. doi: 10.1111/nan.12647.

Wang J, Yu JT, Tan L. 2015. PLD3 in Alzheimer's disease. Mol Neurobiol. 51(2):480–486. doi: 10.1007/s12035-014-8779-5.

Wijte D, McDonnell LA, Balog CI, Bossers K, Deelder AM, Swaab DF, Verhaagen J, Mayboroda OA. 2012. A novel peptidomics approach to detect markers of Alzheimer's disease in cerebrospinal fluid. Methods. 56(4):500–507. doi: 10.1016/j.ymeth.2012.03.018.

Wilson DM, III, Cookson MR, Van Den Bosch L, Zetterberg H, Holtzman DM, Dewachter I. 2023. Hallmarks of neurodegenerative diseases. Cell. 186(4):693–714. doi: 10.1016/j.cell.2022.12.032.

Wright BL, Lai JT, Sinclair AJ. 2012. Cerebrospinal fluid and lumbar puncture: a practical review. J Neurol. 259(8):1530–1545. doi: 10.1007/s00415-012-6413-x.

Wu T, Dejanovic B, Gandham VD, Gogineni A, Edmonds R, Schauer S, Srinivasan K, Huntley MA, Wang Y, Wang TM, et al. 2019. Complement C3 is activated in human AD brain and is required for neurodegeneration in mouse models of amyloidosis and tauopathy. Cell Rep. 28(8):2111–2123.e6. e2116 doi: 10.1016/j.celrep.2019.07.060.

Xiang W, Windl O, Wünsch G, Dugas M, Kohlmann A, Dierkes N, Westner IM, Kretzschmar HA. 2004. Identification of differentially expressed genes in scrapie-infected mouse brains by using global gene expression technology. J Virol. 78(20):11051–11060., doi: 10.1128/JVI.78.20.11051-11060.2004.

Yoshihara M, Montana ES. 2004. The synaptotagmins: calcium sensors for vesicular trafficking. Neuroscientist. 10(6):566–574. doi: 10.1177/1073858404268770.

Yuan P, Zhang M, Tong L, Morse TM, McDougal RA, Ding H, Chan D, Cai Y, Grutzendler J. 2022. PLD3 affects axonal spheroids and network defects in Alzheimer's disease. Nature. 612(7939):328–337. doi: 10.1038/s41586-022-05491-6.

Zárate S, Stevnsner T, Gredilla R. 2017. Role of estrogen and other sex hormones in brain aging. Neuroprotection and DNA repair. Front Aging Neurosci. 9:430. doi: 10.3389/fnagi.2017.00430.

Zelek WM, Fathalla D, Morgan A, Touchard S, Loveless S, Tallantyre E, Robertson NP, Morgan BP. 2020. Cerebrospinal fluid complement system biomarkers in demyelinating disease. Mult Scler. 26(14):1929–1937. doi: 10.1177/1352458519887905.

Zerr I. 2022. Laboratory diagnosis of Creutzfeldt-Jakob Disease. N Engl J Med. 386(14):1345–1350. doi: 10.1056/NEJMra2119323.

Zetterberg H, Bozzetta E, Favole A, Corona C, Cavarretta MC, Ingravalle F, Blennow K, Pocchiari M, Meloni D. 2019. Neurofilaments in blood is a new promising preclinical biomarker for the screening of natural scrapie in sheep. PLoS One. 14(12):e0226697. doi: 10.1371/journal.pone.0226697.

Zhang W, Xiao D, Mao Q, Xia H. 2023. Role of neuroinflammation in neurodegeneration development. Signal Transduct Target Ther. 8(1):267. doi: 10.1038/s41392-023-01486-5.

Zündorf G, Reiser G. 2011. Calcium dysregulation and homeostasis of neural calcium in the molecular mechanisms of neurodegenerative diseases provide multiple targets for neuroprotection. Antioxid Redox Signal. 14(7):1275–1288. doi: 10.1089/ars.2010.3359.